Nat Hazards (2017) 88:431–452
DOI 10.1007/s11069-017-2873-8

ORIGINAL PAPER

Assessment of hydro-geomorphological hazard potentials in the Chilean semiarid coastal range and its impacts on La Serena city, Coquimbo Region

María Victoria Soto[1,2] · Pablo Sarricolea[1] · Sergio Andres Sepúlveda[2,3,4] · Giuliano Rodolfi[5] · Misael Cabello[6] · Michael Maerker[7]

Received: 2 May 2016 / Accepted: 9 April 2017 / Published online: 22 April 2017
© Springer Science+Business Media Dordrecht 2017

Abstract Two micro-catchments, tributaries of the Elqui River in the coastal range of the semiarid central-northern Chile were analyzed to establish the hazard potentials associated with extreme rainfall and their effects on the urban area of La Serena city. Geomorphological mapping was performed identifying the morphological features associated with inherited and present-day processes, through photointerpretation and field work. To assess the geohazard potentials related to extreme precipitation events, a detailed terrain analysis was performed deriving topographic indices that in turn characterize the related process potentials. Extreme rainfall events were calculated with a decadal recurrence (>60 mm/day) and are subsequently associated with El Niño (ENSO) and Pacific Decadal Oscillation (PDO warm phase) events. We applied a simple storm flow model using a 20-year return period reflecting a disastrous flood event that affected the La Serena urban area in June 2011. The results highlight the spatial distribution of the hazard potentials in the two Elqui tributaries and their effects on the La Serena urban area. We show that areas subject to intensive land use change and urban sprawl associated with the lower marine terrace and river mouth of the Elqui River are of very high flooding and tsunami risk.

Keywords Chilean coastal area · Semiarid · Flood hazard potential · Heavy rainfall · Terrain analysis · Hydrological modeling

✉ María Victoria Soto
mvsoto@uchilefau.cl

[1] Department of Geography, University of Chile, Portugal 084, Santiago, Chile

[2] CITRID, Risk Reduction and Disaster Program, University of Chile, Santiago, Chile

[3] Department of Geology, University of Chile, Santiago, Chile

[4] Institute of Engineering Sciences, University of ÓHiggins, Rancagua, Chile

[5] University of Florence, Florence, Italy

[6] Physical Geography Lab, Department of Geography, University of Chile, Santiago, Chile

[7] Department of Earth and Environmental Sciences, University of Pavia, Pavia, Italy

1 Introduction

As stated by Cardona (2009), natural risks are considered an unresolved socio-environmental problem. However, potential hazards related to social and environmental changes caused by global climate change may also be considered as unresolved phenomena. These changes constitute a new challenge in the study of natural risk and require a detailed assessment and adaption of scenarios for global climate change for a proper risk prevention or risk reduction (Lei and Wang 2014). Over the last two decades, approximately 76% of the global catastrophic events were of hydrometeorological origin (EIRD 2008). In the period between 1900 and 2013, flooding was the most frequent natural disaster, affecting more people than any other event of natural origin (Banks et al. 2014).

Similar to social structures, landscape processes underwent continuous spatiotemporal changes; therefore, they are dynamic and interactive phenomena that often are not adequately studied. These processes are associated with hazards of natural origin; thus, an analysis from a dynamic perspective allows for an improved assessment of risks (Aubrecht et al. 2013). To evaluate the different types of hazards, analysis scales, magnitudes of measurements and associated risk conditions must be considered. Kappes et al. (2012) formulated the concept of multirisk, which is linked to environmental changes and human impact and constitutes an agent of change in processes and behavior of morphological systems (Keiler et al. 2012; Birkmann et al. 2013).

Arid and semiarid environments are morphological systems that are highly sensitive to climate variability, e.g., as extreme precipitation events causing soil erosion. Such events were analyzed by Owen et al. (2011) for the Atacama Desert and the Chilean semiarid coast. Semiarid environments are complex systems under a climatic, ecologic, hydrologic and socioeconomic point of view, particularly when they are subject to climate change and anthropic interventions that are typical of the Anthropocene period (Wilcox et al. 2011). To mediate such changes, the growth of cities must be considered, because they are supposed to receive 60% of the global population in the next 50 years, which in turn will impact the consumption of natural resources and the transformation of environmental systems (Huang et al. 2010).

The Chilean semiarid coastal environment is vulnerable to new environmental impacts that came up in this century. Some of these impacts are modeled using scenario analysis developed by the National Environment Commission of Chile (CONAMA, initials in Spanish 2006) and Garreaud et al. (2008). These models predict an increase in precipitation and temperatures in Andean catchments that will result in concentration of episodic rainfall and, hence, in flood hazards. Additional important phenomena that occur along the Chilean semiarid coast are the El Niño-Southern Oscillation (ENSO) phenomenon (El Niño, La Niña) and the Pacific Decadal Oscillation (PDO, Sarricolea and Martín-Vide 2012). El Niño event is detected by standardized differences in sea-level pressure at the Tahiti and Darwin observatories and are also detected by positive anomalies of sea surface temperature in delimited areas of the equatorial Pacific (usually El Niño 3.4 region). The 1983 El Niño event was identified by warm phases of PDO and the El Niño 3.4 region (but not with a negative Southern Oscillation Index, SOI, which occurred in 1982). However, the El Niño event of 1997 and 2015 recorded both types of indices (PDO and SOI).

Previous works on the semiarid areas of Chile illustrate that such precipitation events are related to geohazards through the activation of geomorphological processes in microcatchments generating hyper-concentrated flows, floods and flashfloods (Castro et al. 2009; Märker et al. 2012; Soto et al. 2010, 2012, 2015).

The city of La Serena sited in the Coquimbo Bay (29°S/70°W) is the second oldest city in Chile. It was founded in 1544 on a high marine terrace near the Elqui River, which drains the fertile soils of the adjacent valley. Currently, the city has 486,000 inhabitants (National Statistics Institute of Chile, INE, initials in Spanish 2012), and it is an important hub for services, lodging and tourism for central-northern Chile and the Chilean semiarid coast. The study area includes the Coquimbo Bay coastal urban and future expansion urban areas (Fig. 1).

Over the last three decades, La Serena was subject to intense urban growth and real estate development processes (Ortiz et al. 2002; Castro and Ortiz 2003; Ortiz and Escolano 2005). Such growth initially occupied the high marine terraces and later extended toward the coastal flats. Currently, urban growth is directed toward the lower fluvial terraces and hence leads to an increased risk for population and infrastructure. Soto et al. (2015) established that general hazard conditions occur in the urban area, and they are associated with hydrometeorological phenomena, such as floods and landslides.

In the context of the existing hazards and urban expansion processes in the La Serena area, Ortiz et al. (2011) concluded that there is hardly any awareness of the risk associated with endogenous (earthquake and tsunami) and exogenous hazards (floods and mudslides) among the city's inhabitants. This lack of awareness is also found among the tourists that visit the coastal area (Wyndam 2012). Among others, this finding explains the intense population growth along the coastal belt and on the lower fluvial terrain. The fluvial terraces were analyzed by Sarricolea (2004) and associated with flood hazards and risks related to the poor drainage characteristics of the soil. The lowest marine terrace

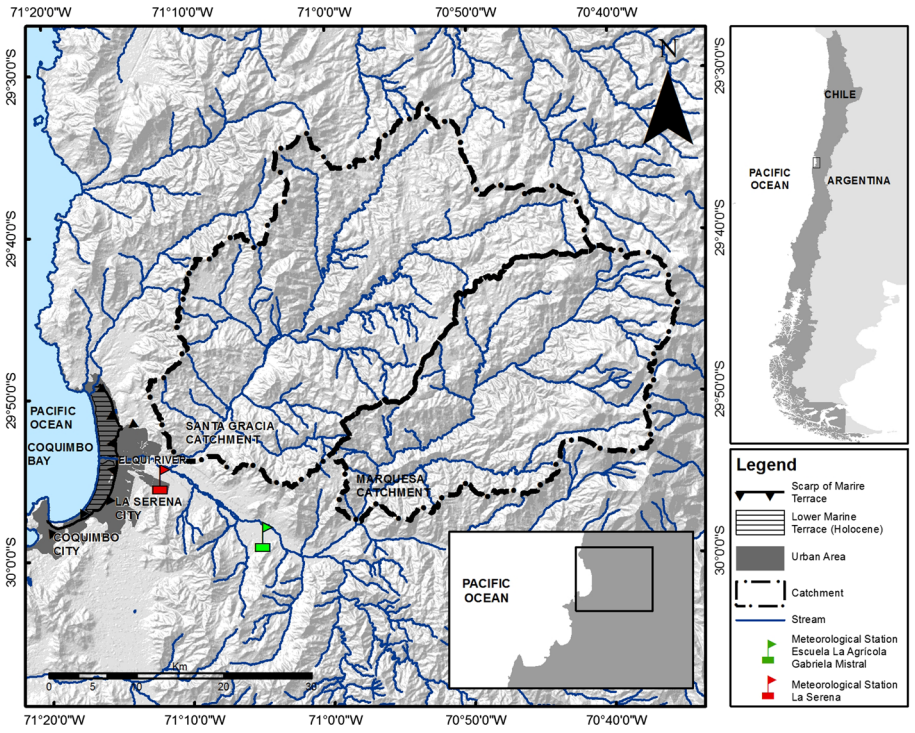

Fig. 1 Study area, showing the Marquesa and Santa Gracia catchments, and the La Serena city area

corresponds to remnants of barrier beaches, swamps and dunes (Soto et al. 2015) that were drained for the constructions of houses, roads and tourist resorts.

The purpose of this research is to identify and assess the hydrometeorological geohazards affecting the study area. Particularly, we focus on the identification of the flood-prone areas in zones that are subject to urban expansion, based on geomorphological, meteorological, and terrain analyses and the study of the influence of ENSO. The flood conditions in the lower La Serena region are geographically analyzed taking into account two catchments (Marquesa and Santa Gracia) that drain directly into the Elqui River downstream the Puclaro Reservoir, which regulates the river flow from the upper Andes. During the El Niño events of 1983 and 1997, these catchments contributed important flow rates to the main system, and the flow reached the mouth of the central part of the lower marine terrace, currently subject to extensive urban expansion. Therefore, we hypothesize that during precipitation events that are equal to, or greater in magnitude than those experienced in previous strong El Niño years, the city will be affected by floods generated in the Elqui tributaries of the Marquesa and Santa Gracia torrents.

2 Regional setting

2.1 Tectonic setting

The study area is located in a low-angle subduction segment of the Nazca plate beneath the South American plate, with historic seismicity (Pardo et al. 2002a). Before the recent 2015 earthquake, the last large interplate earthquake in the region was an M 7.9 in 1943 (Illapel earthquake), and previous ones in 1647, 1730 and 1880, normally with associated tsunami. An intermediate depth intraplate earthquake was registered south of La Serena in 1997 (Punitaqui earthquake, M 7.1; Pardo et al. 2002b). The zone is known as a seismic gap. Recent studies of seismicity and crustal deformation suggested that the region was being loaded for a large interplate earthquake in the near future (Vigny et al. 2009). In fact, on September 16, 2015, a large M 8.4 interplate earthquake with epicenter about 190 km south of La Serena caused light damage on city buildings, but severe damage on adobe housing especially in Hinterland towns and villages of the region. The earthquake triggered a moderate tsunami with waves running up to about 4.5 m (ONEMI 2015) that mainly affected coves and small coastal villages and parts of the city of Coquimbo and La Serena along the shoreline. According to a Gutenberg–Richter law presented for this area by Soto (2016), the return period for interplate earthquakes of magnitude over 6.0 is of a few years, while for large earthquakes of magnitude over 8.0 is over 100 years. The region has geological and historic records of tsunami (Le Roux and Vargas 2005; Beck et al. 1998), increasing the risk especially in some flat areas prone for flooding such as the coastal area of La Serena and Coquimbo, as was observed during the 2015 earthquake.

2.2 Geological and geomorphological setting

La Serena is located in a system of marine and fluvial terraces adjacent to the coastal range that is composed of volcanic sedimentary rocks from the lower Cretaceous. The Coquimbo Formation lying over this basement corresponds to a series of marine and scarcely consolidated sediments (Moscoso et al. 1982) in turn forming marine terraces. The origin of these terraces is attributed to glacio-eustatic and tectonic movements (Le Roux et al. 2006; Saillard et al. 2009, 2011). Paskoff (1970) identified five levels of marine terraces in the

Coquimbo Bay (Middle–Upper Pliocene and the Pleistocene and Holocene). These levels correspond to fossil beach deposits separated by paleocliffs, and the terraces reach 130 m.a.s.l.

The Elqui River is a high Andean catchment and its flow rate is regulated for the last two decades by the Puclaro Reservoir (Fig. 2). However, the presence of non-regulated coastal mid-mountain tributary catchments below the Puclaro Dam is important when analyzing future floods associated with significant precipitation events, such as strong El Niño events, which have not occurred since 1997. The two largest tributaries supposed to have major effects on the downstream coastal areas are the Santa Gracia (1073 km^2) and the Marquesa catchment (737 km^2, Fig. 1).

2.3 Climatic conditions

This region is located in a climatic transition zone of desert and Mediterranean climates and is classified as a semiarid climate with abundant coastal clouds. Recently, Sarricolea et al. (2016) classified the climatic conditions as Koppen–Geiger, namely a cold semiarid climate with dry summers and oceanic influences, which reaches until about 25 km inside the Elqui Valley. Following the meteorological time series (1980–2013), the foggy coastal areas present 87% humidity in the morning (08:00 a.m) due to the cold Humboldt Current. Moreover, they are characterized by moderate temperatures (13.7°) and very low thermic

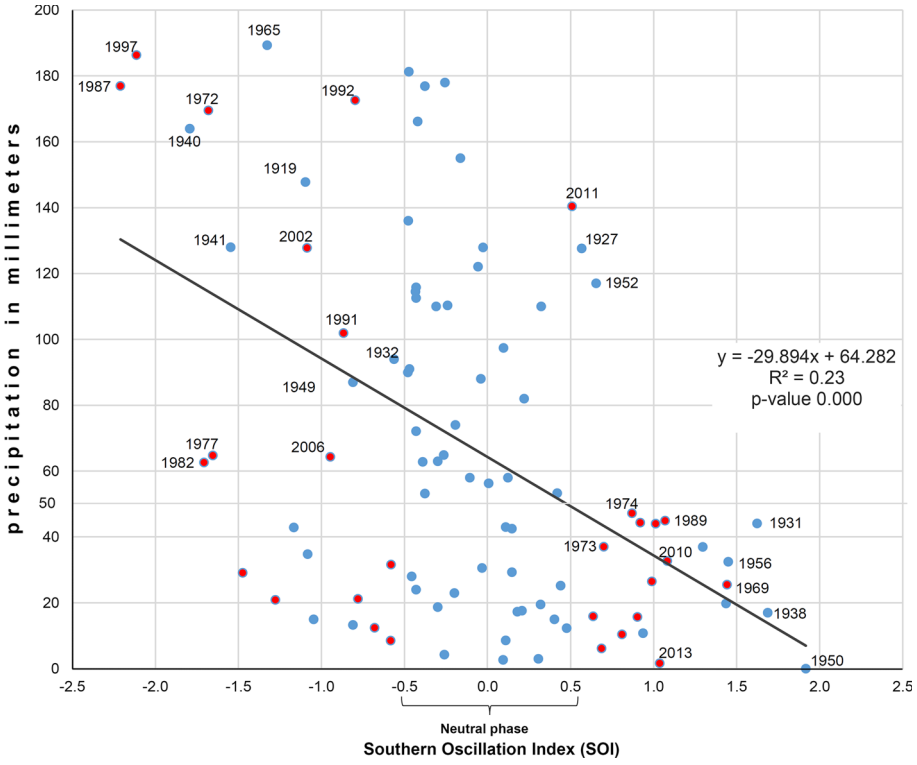

Fig. 2 Correlation between SOI of MJJ and the rainfall of JJA for the period 1919–2013. The *blue points* represent the period 1919–1966 and the *red* one the period 1967–2013

amplitudes. The annual average rainfall is approximately 79.1–104.4 mm; however, the amount of rainfall increases substantially during El Niño events (116.8 mm in 72 h, in 1983; 109.6 mm in 1987; and 130.2 mm in 1992) and is concentrated in just a few days. The 2015 El Niño event has recorded 53.1 mm between July and August, with a peak rainfall in 24 h of 29.7 mm (July 12, 2015).

3 Methods

The assessment of different geo-hydrological hazard potentials in the study area is conducted throughout detailed terrain analyses, geomorphological mapping, hydrological modeling, as well as rainfall data analyses.

3.1 Climatic analysis

We analyzed the daily rainfall time series of La Serena weather station (29°55′S–71°12′W, 142 m.a.s.l., Fig. 1) from 1919 to 2013 in terms of extreme events for 24, 48, 72 and 92 h intervals. Especially the 2, 3 and 4 days events contribute significantly to soil saturation, surface runoff and are also triggering of landslide processes. Further, for the 2015 event rainfall data from Gabriela Mistral station (29°58′42.67″S–71°4′49.39″W, 198 m.a.s.l., Fig. 1) were used.

The hydrological dynamics of the study area were characterized using two different approaches. The first one analyzes the effects of the ENSO phenomenon during the rainy season (June, July and August), using direct and linear correlations and a month lag time. The second approach assesses the maximum rainfall recurrence in 1, 24, 48, 72 and 96 h. For 1-h recurrence calculations, Vargas (1999) expressions were applied, and for 1–4-day recurrence a frequency distribution model was used.

To investigate the ENSO phenomenon, the Southern Oscillation Index (SOI) achieved from the Climatic Research Unit of University of East Anglia was applied on a monthly basis. For the assessment of the maximum precipitation return periods, we used daily data from the Meteorological Service of Chile based on yearbooks available since 1919, the start of continuous observations, and on digital data from 1961 onwards.

For the analysis of the precipitation events, we employed an extrapolation procedure. For calculating the return periods, the Gumbel function was used, which has two parameters, u and α corresponding to the shape and scale parameters, which were obtained from the mean and standard deviation as illustrated by the following expression:

$$f(x) = \exp(-\exp(-((x-u)/\alpha)))$$

The Gumbel function, it is given as follows:

$$T = \frac{1}{1 - f(x_T)}$$

3.2 GIS analysis

Topographic indices can be used as proxies to assess the susceptibility for certain geohazards as well as to derive information on forms and features reported in traditional

geomorphological maps. In this study, we used slope- and catchment area-based topographic indices to describe the present-day fluvial and slope process potentials (Märker et al. 2008, 2011; Zakerinejad and Märker 2014). On the other hand, we derive basic information for the geomorphological map like terrain characteristics such as slope, curvatures and exposition as well as more complex indices describing fluvial terraces and erosion base levels.

Concerning the slope and fluvial processes, we used the Stream Power Index (SPI) (Eq. 1) as a measure of the erosive power of linear concentrated water flows or streams. It is an index illustrating the available energy for deep linear incisions that are normally related to turbulent flows.

$$\mathrm{SPI} = A_s * G \tag{1}$$

with A_s = specific catchment area and G = slope gradient.

The Transport capacity Index (TCI) (Eq. 2) yields information on the general capacity to transport material. This index or variations of it are also applied in erosion models like RUSLE (Renard et al. 1997) or USPED (Mitas and Mitasova 1998). TCI is derived as follows:

$$\mathrm{TCI} = A_s^m * (\sin G)^n \tag{2}$$

with m and n exponents describing different surficial erosion processes. Prevailing rill erosion processes are related to $m = 1.6$, $n = 1.3$ while for prevailing sheet erosion is related to $m = n = 1$. Here, we are interested in the sheet erosion processes and hence used for m and n the value 1.

The Topographic Wetness Index (TWI) describes the spatial distribution of soil humidity according to terrain morphology, and hence, also on potential runoff after precipitation events due to saturation excess. Additionally, high TWI values especially on mid and foot slope positions with concave-shaped slopes indicate an elevated landslide potential because of the higher weight of the saturated substratum (Montgomery and Dietrich 1994a, b; Tucker and Hancock 2010).

$$\mathrm{TWI} = \ln(A_s/G) \tag{3}$$

The modified catchment area (MCA), the vertical distance to river network and the altitude above stream channel network (AACN) deliver information about the spatial configuration of flooding areas. These indices were derived following Olaya and Conrad (2009). The AACN is also called isobase map (Grohmann 2004). Basically, the AACN reflects the elevation model corrected by the channel net base level. This index reveals also fluvial terrace systems that are reported in the geomorphological map.

3.3 Hydrological modeling

In order to assess single storm flow events with a certain hazard potential, we used a simple Soil Conservation Service (SCS) runoff curve number approach (CNII) (Hawkins et al. 2009). The model was implemented in the System for Automated Geoscientific Analyses (SAGA) (Conrad 2006; Olaya and Conrad 2009, Boehner et al. 2002) to model storm flows and water volumes and, hence, to estimate the flooding areas. This approach yields the spatial distribution of the maximum runoff for a given precipitation event and certain land use and soil infiltration characteristics. For the GIS-based hydro-geomorphological analysis, we utilized an ASTER GDEM Digital Elevation Model (DEM) with a 25-m

resolution. The study area is characterized by a scarce vegetation cover and a homogeneous geologic substrate with a shallow soil cover. The soil of the area shows very little or no infiltration especially after long dry periods (Märker et al. 2012). During fieldwork, we conducted infiltration tests and observed hydrophobic effects especially on soils with quite high organic matter content. Thus, we set the soil- and vegetation-related CN values to a maximum in order to get the maximum runoff that might occur for a given precipitation event.

3.4 Geomorphological analysis

The geomorphological map yields important information on the geomorphological forms and features, in turn result of the related processes. We conducted geomorphological analyses of the two tributary catchments of the lower Elqui River, namely the Santa Gracia and the Marquesa (Fig. 1) catchments. A geomorphological map was generated according to the hillslope systems defined by Araya-Vergara (1985) and adapted to semiarid environments (Soto et al. 2010, 2012). The landscape is particularly characterized by the relationship between hillslopes determined by their lithology and the potential mass contribution to the stream network. The geological information was extracted from Emparán and Pineda (2006). Fluvial terraces, alluvial fans and glacis were mapped based on stereo-photointerpretation and validated by field surveys in January 2014 and January 2015.

Moreover, we estimated the Tsunami hazard using a simple GIS overlay procedure based on Tsunami wave heights provided by the Servicio Hidrografico y Oceanografico de la Armada de Chile (SHOA).

4 Results

4.1 Rainfall analysis

The environmental changes modeled for the Andes in the Elqui River, such as increased concentrations of precipitation and reduction in the 0° isotherm (Garreaud et al. 2008), are not relevant for the analysis of floods in the mid- and lower section of the Elqui valley because of the regulating action exerted by the Puclaro Dam. However, strong and intense episodic precipitation events that may occur in the coastal zone may have an impact on the La Serena city because the analyzed catchments drain directly to the Elqui River crossing through the city.

The annual average rainfall of La Serena is 95.9 mm (1919–2013), which had a significant decrease (p value = 0.01), estimated to 6 mm/decade. The wettest year of the series was 1919 with 306.6 mm total precipitation, and the driest year corresponds to 4.3 mm in 1962. The winter rainfall (June, July and August, JJA) represents 70% of the annual rainfall.

For the JJA correlations of the precipitation amounts, the SOI of the same period and lag times of 1, 2 and 3 months back and forth were tested. The results indicate that JJA precipitation is best correlated with the SOI and a lag time of 1 month (May, June and July) showing a Pearson correlation coefficient of 0.479 and a p value of 0.0 implying high statistical significance. Figure 2 shows the precipitation of the winter months (JJA) and its correlation with the 1-month lag SOI (MJJ). Precipitation is higher during El Niño and

below normal during La Niña. Events at a threshold of 50 mm are associated with El Niño (15 occurrences), with the exception of the years 1927, 1952 and 2011, which are associated with weak La Niña conditions. It should be noted that the winter precipitation of 2011 was due to a negative anomaly of the Antarctic Oscillation.

Another interesting fact shown in Fig. 10 is that the frequency of ENSO phenomena has become more persistent in the latter half of the series. El Niño events 1967–2013 exceeded the threshold of 50 mm are 9 out of 15 (60%). In the case of La Niña events, during the second half of the series (1967–2013) this type of anomaly predominated with 13 cases out of the 20 of the whole series (65%). This means that despite a decrease in rainfall amounts, extreme events have become more frequent over the last 50 years and consequently rainfall concentration increased, in particular for El Niño events.

Major events up to 60 mm/24 h are observed in 11 cases in the last 95 years with a return period of 9.9 years according to the Gumbel distribution, which means a decadal recurrence (Tables 1, 2, 3). Table 2 shows the results of the calculation of the return periods between 5 and 120 years, the maximum return period.

In the cases of 2, 3 and 4 days (Table 3), an increase in precipitation records is observed in comparison with 24 h cases. In the La Serena region particulary cold frontal systems affect the area for consecutive days, increasing the amounts of total precipitation. Events with 100 mm/24 h have a 100-year frequency, but might occur with a recurrence interval of 20 years, with 96 h of consecutive precipitation.

4.2 Terrain analysis

The terrain analysis describes the structural and palaeo-landscape features of the study area through the AACN Index, which is shown in Fig. 3. The index illustrates the Miocene terraces as well as the younger Holocene ones. In addition, this index highlights the marked NNE-SSW trending Andean tectonic incidence in the geometry of the drainage network and the distribution of deposit formations associated with the valley systems. The same index shows also the potential flooded areas in blue.

Topographic indices yield also information about the spatial distribution of soil erosion and landslide susceptibility as major contributing sources for sediments in the river system. The SPI is a measure of the erosive power of concentrated linear water flows or streams.

Table 1 Precipitation events up to 60 mm/day in La Serena for the period 1919–2013

Year	Maximum rainfall in 24 h	Teleconnections associated
1919	64.8	El Niño anomaly
1927	80.9	
1929	60.8	
1938	89.2	
1941	73.0	El Niño anomaly; PDO warm phase
1957	100.0	El Niño anomaly; PDO warm phase
1972	66.7	El Niño anomaly
1983	69.5	PDO warm phase
1984	62.8	PDO warm phase
1987	104.7	El Niño anomaly; PDO warm phase
2001	74.1	

Table 2 Return period (Gumbel distribution) of daily precipitation and hourly maximum values for La Serena between 1919 and 2013 according to Vargas (1999)

Return period (years)	Maximum rainfall in 24 h (mm)	Maximum rainfall in 1 h (mm/h)
5	47.9	10.3
10	60.2	12.9
20	72.0	15.5
50	87.2	18.8
100	98.7	21.2
120	101.7	22.0

Table 3 Return period (Gumbel distribution) of maximum rainfall in 2, 3 and 4 days in La Serena 1961–2013

Return period (years)	Maximum rainfall in 48 h (mm)	Maximum rainfall in 72 h (mm)	Maximum rainfall in 96 h (mm)
5	55.3	58.7	62.6
10	70.3	75.4	80.9
20	84.7	91.5	98.5
50	103.4	112.2	121.2

Figure 4 shows the areas prone to incision in orange (medium) and red (strong). The lower parts of the two study catchments do not show any signs of incision suggesting a low-energy flow domain with braided river morphologies and depositional processes.

The TCI reveals the potential for surficial rill–interrill erosion. As shown, the steeper slopes of the upper Marquesa and the middle Santa Gracia catchment are characterized by quite high erosion potentials. These relatively high topographic potentials for surficial erosion may lead together with the scarce vegetation cover and erodible substrates to a quite big sediment delivery toward the fluvial channel and may explain the hyper-concentrated flows observed during the extreme event in 1997. The spatial distribution of TCI is illustrated in Fig. 5.

The TWI characterizes the catchment areas where saturation runoff may occur due to the concentration of water and low slopes leading to soil saturation (Fig. 6). Moreover, a certain landslide potential can be observed in the lower slope sections of the upper catchments where water concentration is leading to additional weight of the substrates or soils that may lead to mass movements especially if wet conditions (e.g., snow melt) and earthquakes act as triggering mechanisms.

4.3 Geomorphology and geohazard potential of the study area

The Elqui River tributaries, namely the Santa Gracia and Marquesa catchments (Fig. 7a–c), are located in the northern part of the lower Elqui Valley. They are small tributary catchments with outflows located 9 km and 34 km from the mouth of the Elqui River. The catchments exhibit a complex geomorphology associated with forms that were inherited from more humid climates and are characteristic of the Chilean semiarid environment (Paskoff 1970; Soto et al. 2014). These characteristics are shown in dissected slopes and catchments that result from water erosion and alluvial morphologies, such as alluvial fans and alluvial terraces. These relationships were established through absolute dating (Paskoff

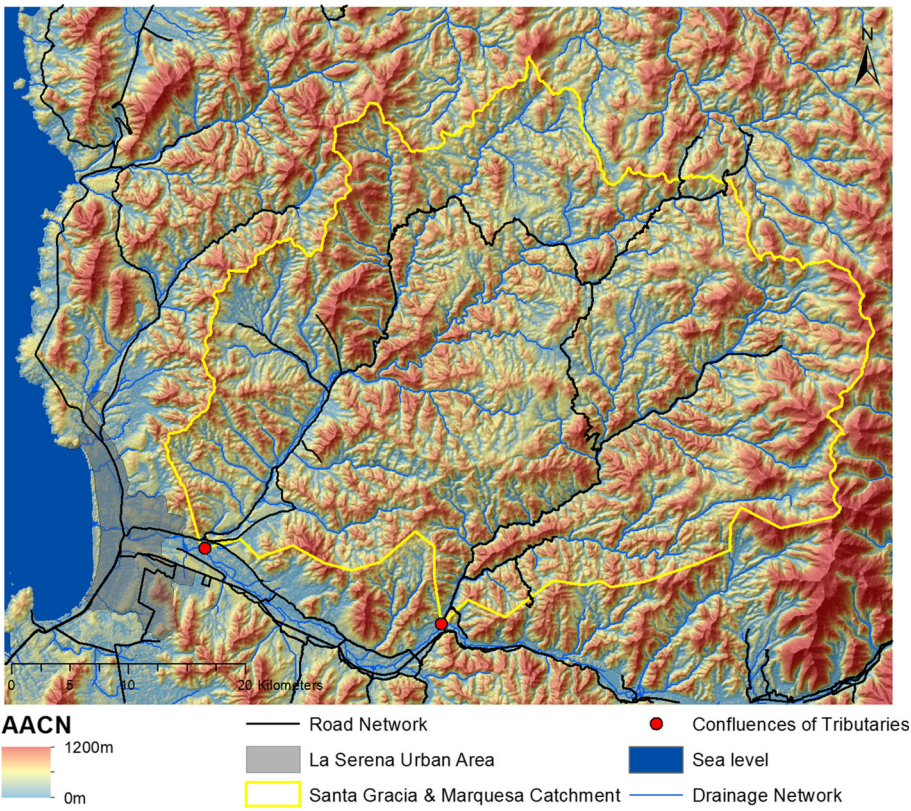

Fig. 3 Altitude above channel network (AACN) (m)

1970; Emparán and Pineda 2006) and field evidence from palaeo-soils identified in slope- and fluvial sequences of both catchments and also in areas further south (Soto et al. 2014) and north (Soto et al. 2015; Soto 2016), along the coastal range of Coquimbo Megabay.

The slope systems correspond to a predominantly plutonic rock lithology with detritic-volcanic sequences from the Cretaceous (Moscoso et al. 1982). These systems are found in both catchments along with an abundance of material deposited at the surface, especially in areas that have experienced hydrothermal alteration where significant assemblages of rock chaos occur along with the presence of tors (Fig. 8). In turn, volcanic rock relief appears as folded hillslopes that expose the different rocky strata in terms of thick outcrops accompanied by alluvial fans and detritic slopes in the lower areas (Fig. 7a, b).

Geomorphologically, the conditions of the plutonic slope systems with rock chaos, hydrothermal alteration and abundant material exposed to weathering processes have contributed to a significant mass transfer from the upper areas of the mountain systems. These folded mountain areas of the upper Marquesa catchment exhibit structural plateaus and homoclinal slopes systems. It is worth highlighting that this section of the catchment is located in the nival environment and, as a result, landslides and general morphological manifestations of snow have been identified, including the linear dissection of the slopes.

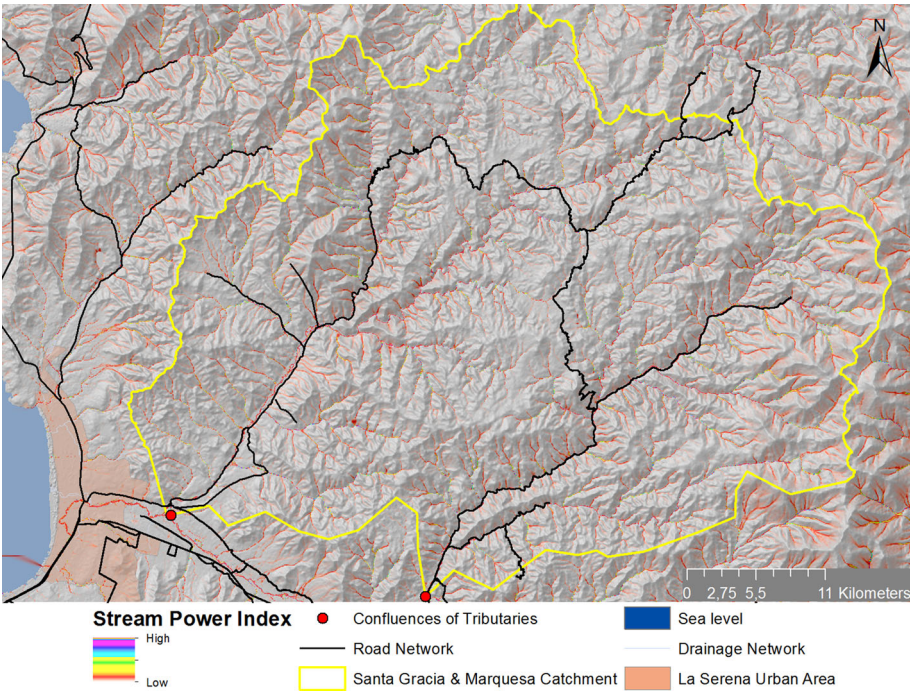

Fig. 4 Stream Power Index (SPI): In *orange* and *red areas* prone to deep linear erosion and fluvial erosion processes

Regarding the deposit features, the alluvial fans exhibit a characteristic location, laterally oriented toward the main valley. These alluvial fans are of a torrential nature, have a convex profile and show the presence of a dissected main channel. Their characteristics indicate the episodic activity of the processes associated with intense hydrometeorological events. The latter often generate hyper-concentrated flows that have the capacity to drag debris and blocks from the slopes that subsequently are deposited in the distal regions of the modern alluvial fans (Fig. 7a, b).

The main streambeds of the tributaries of both catchments exhibit a braided pattern in wide beds (>500 m) in which there is evidence of water action resulting from the pattern of channels, sand banks and gravels, which are well developed and preserved. The streambeds normally develop during the last significant precipitation events (Fig. 9). Local inhabitants stated (fieldwork January 2015) that in 1997 the Marquesa and Santa Gracia catchments were active the last time, completely flooding their streambeds (Fig. 10).

The stream valleys exhibit very deep incisions that are associated with the landscape inherited from the Pleistocene. However, there is also evidence of a high erosion and incision potential of the current beds. In the sub-catchment of Santa Gracia catchment, a bed was identified that was highly incised by floods caused by the El Niño event of 1997 (Fig. 11). The degree of incision is higher than the ancient elevation differences between the terrace escarpments and the channels. We also observed in the field some incised lateral deposits corresponding to an alluvial fan, which in 1997 became a terrace cone. Although terrace cones of this semiarid Chilean region are generally attributed to the paleo-landscapes of the Pleistocene valleys, their dissection can be attributed to recent processes

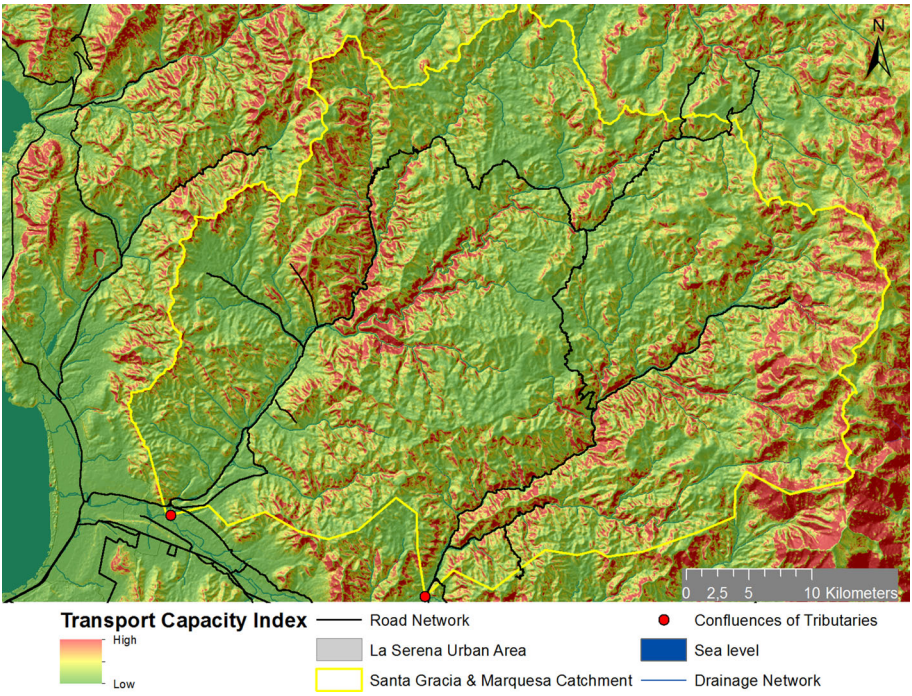

Fig. 5 Transport Capacity Index (TCI): In *red areas* with high erosion potential in *green areas* with no potential and in *yellow areas* with low erosion potentials

(Paskoff 1970). Therefore, we can hypothesize that a further dissection of the landscape will continue during the next decades.

The geomorphological dynamics, along with the seismic activity, of both micro-basins explains the conditions of abundant detrital sedimentary materials available on the slopes, ravines, and in river beds that feed the flooding processes associated with extraordinary rainfall events.

4.4 River floods and flash flood

Based on the last river flood of 1997, the river is expected to cause flooding for similar rainfall events. Such flooding might be accompanied by hyper-concentrated flows from the sediment-rich head catchments and slopes. However, in 2011, there was an exceptional precipitation event with 70 mm in 24 h. The flooded areas concentrated in the urban sector of the Holocene marine terrace, an area that is experiencing intensive urban expansion. In the Santa Gracia and Marquesa catchments and Elqui riverbed, no floods were observed because it was only a 24-h event and infiltration was too high.

As shown above, the TWI (Fig. 6), representing the soil saturation capacity and hence surface runoff potential, illustrates the spatial distribution of saturated areas after long precipitation periods. In the blue areas, soils are usually saturated and produce saturation excess runoff.

The MCA provides an approximate estimation of potentially flooded areas during extreme rainfall events and was used to model the maximum river runoff for a 70 mm/24 h

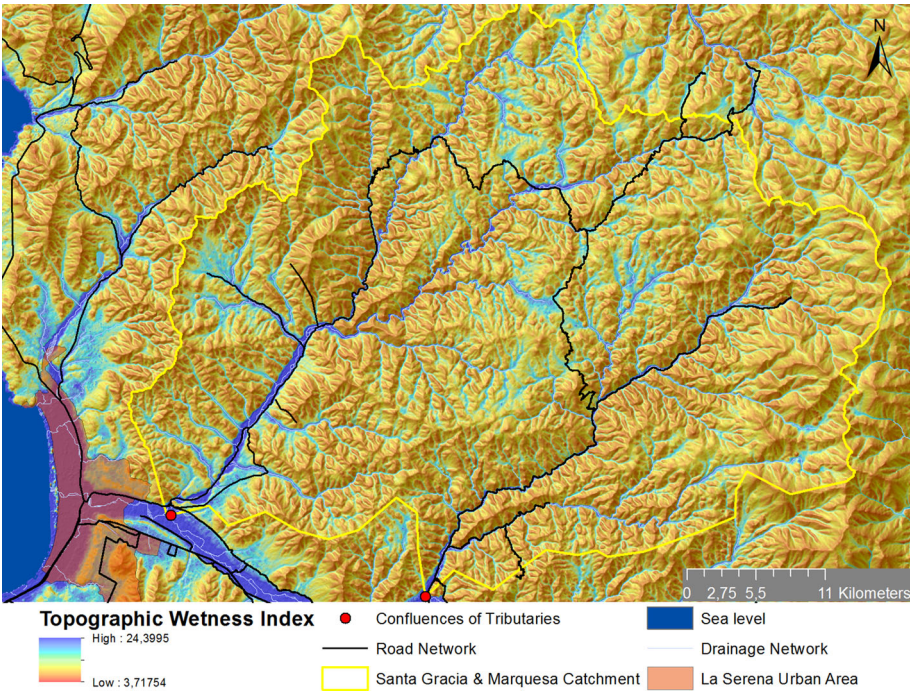

Fig. 6 Topographic Wetness Index (TWI): In *blue areas* with higher moisture, in *brown dry areas*

event such as the one that occurred in 2011 (Fig. 12). Although the potential flood area for a 70 mm/24 h event is large, this scenario becomes even more likely with successive precipitation events on top of already saturated soils. This situation occurred, e.g., during the El Niño events of 1983 and 1997. The validation of the model of the modified Santa Gracia catchment is shown in Fig. 10b, indicating the maximum height reached by the flood of 1997. The distal section of the Santa Gracia catchment exhibits a marked narrowing with a width of approximately 40 m, which constitutes a natural obstruction in the catchment leading to a pronounced valley floor flooding (Figs. 5, 7b).

During the March 25, 2015 event, with a rainfall below the magnitude of extreme events described for the Santa Gracia catchment, a moderate flash flood affected the catchment (Fig. 13). Rainfall records in the closest station (Gabriela Mistral/CEAZA, Fig. 1) show a precipitation of 21.3 mm/24 h and a concentration of 7.1 mm/h (14:00 local time). This rainfall event occurred at the end of the driest summer of the last decade and was mainly characterized by surface runoff and minimal to no infiltration at soil surface. This fact may be explained by the soil conditions characterized by high clay content and low permeability crusts formed by the dry climate, impeding infiltration as observed by Märker et al. (2012) for micro-catchments in the Chilean semiarid region (soil hydrophobic effect e.g., Soto 2016; Doerr et al. 2000). The Elqui River bed was flooded in its full cross-sectional extend.

Using the hydrological soil groups identified by Sarricolea (2004) and superimposing a DEM and the MCA index (Fig. 12), it was possible to identify areas that are topographically and pedologically vulnerable to flooding caused by high discharges of the Elqui River or poor soil drainage when intense and concentrated precipitation events occur (infiltration excess runoff). Figure 14 shows the flood-prone areas caused by specific topo-

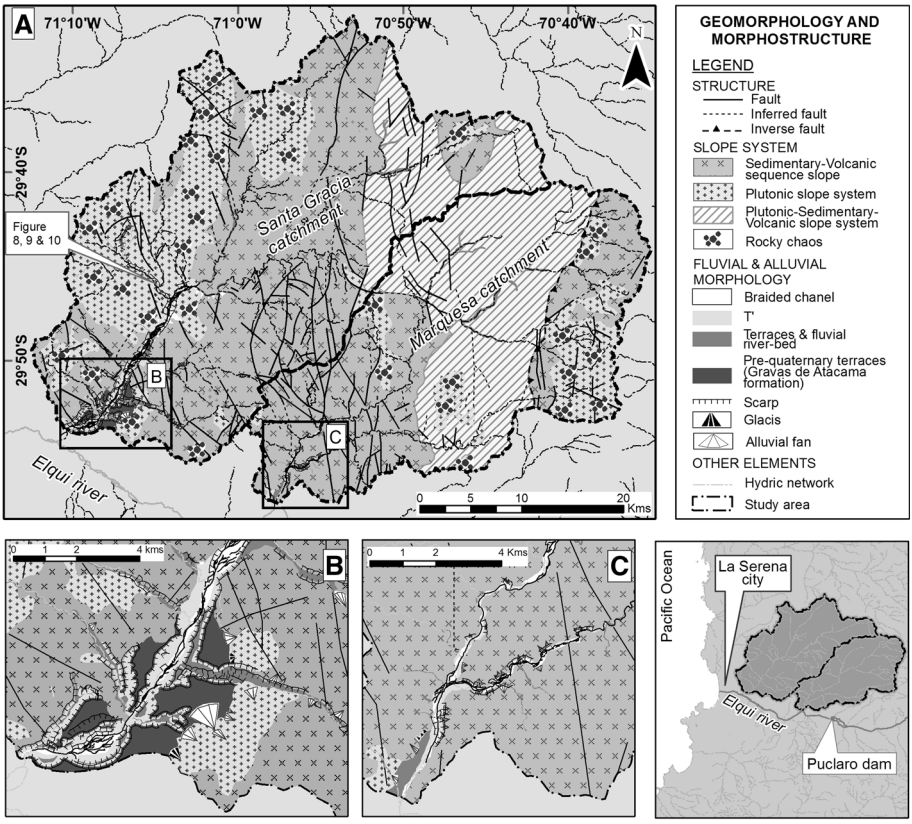

Fig. 7 Geomorphologic map of the study area. **a** Lithology and tectonics of the study area **b** detail of the confluence of Santa Gracia and Elqui River catchment. The presence of river terraces of the Miocene and Pleistocene, with *marked* escarpments due to tectonic uplift. **c** Details of the confluence of Marquesa catchment

pedological conditions (Soto et al. 2015). These areas coincide with the remnants of swamp.

For the 2011, 70 mm/24 h event, the model yields a quite large flooded area. However, this result shows the maximum area flooded since the model was run with the maximum total runoff value. The event of 2011 allows for a partial validation of the model because differential responses occurred according to the geomorphological unit being analyzed. In the Elqui riverbed, the model cannot be validated because the infiltration was very high and no floods or significant flow level rises were recorded. However, a significant subsurface flow can be supposed. Along the coastal zone, the lower marine terrace experienced floods of up to 1 m that remained for at least 24–48 h. This ponding occurs due to saturation and very low infiltration rates of the soils as well as the very slow runoff due to the flat terrain. This situation was also experienced in 2003 during an isolated precipitation event that flooded the same areas as in 2011.

When superimposing the areas characterized by poor soil drainage and flooding over the legally approved land use map of the city of La Serena, the current and potential risk associated with the area's urban growth process can be identified (Fig. 15). According to

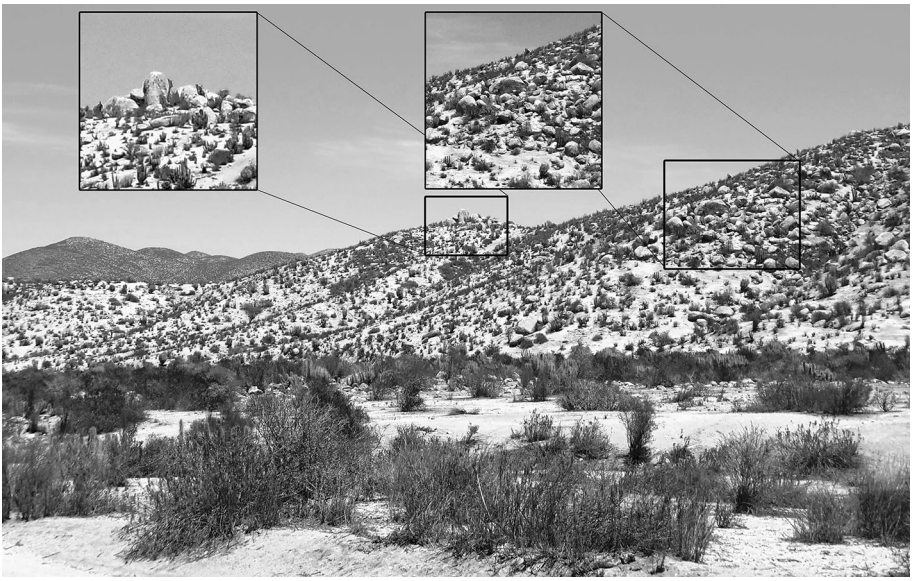

Fig. 8 Rock chaos and tors. Plutonic slopes in Santa Gracia catchment (Fig. 7)

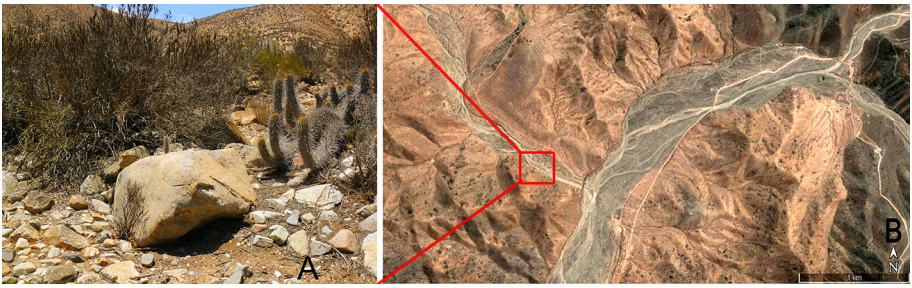

Fig. 9 Braided pattern in the Santa Gracia catchment. **a** Detail of the banks with blocks and rounded and sub-rounded gravel associated with the transport of spheroidal blocks from the slopes with rock chaos. **b** A braided river bed in a torrential catchment

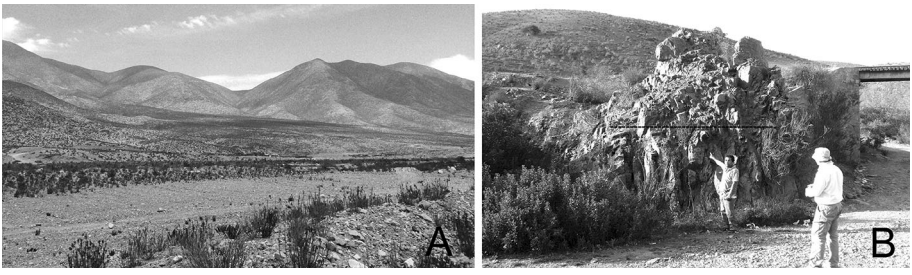

Fig. 10 Flooded area of the Santa Gracia catchment. **a** Mid-section of the catchment, with a braided pattern and bed amplitude of 440 m. **b** Distal section in the proximity of the confluence with the Elqui River. A local inhabitant indicates the height reached by the flood of 1997

Fig. 11 Stream bed of the Santa Gracia creek, associated with a hyper-concentrated flow that occurred in the year 1997. The flow excavated the braided bed of the sub-catchment and dissected an ancient alluvial fan. The thickness of alluvial sequence is 5 m (Fig. 7)

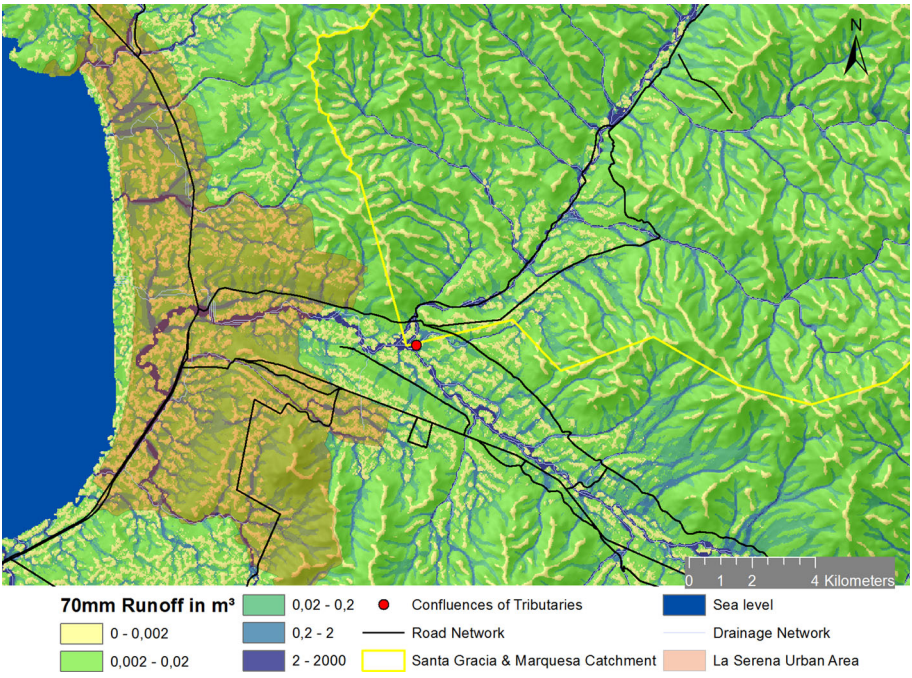

Fig. 12 Maximum river runoff of a 70 mm/24 h event in the La Serena urban area

planning documents (La Serena Communal Regulating Plan), residential, sanitary and infrastructure urban land uses are allowed in areas with potential flood risk.

Currently, there are still many areas that have not been developed for urban use and are instead allocated for agriculture and recreation (country club and golf course) or are awaiting development.

Fig. 13 Flash flood in Santa Gracia catchment on March 25, 2015, associated to a 21.3 mm/24 h rainfall event (not an ENSO event). Photo: Mr. F. Muñoz

Fig. 14 Flooded areas at University of La Serena on the lower marine terrace after 70 mm/24 h rainfall in 2011. The flooding is a consequence of poor infiltration characteristics of the soil. *Source*: www.emol.cl

The urban area affected by river floods is also prone to tsunami flooding as occurred on September 16th, 2015. This tsunami was associated with an interplate earthquake of 8.4 M, located 100 km south of La Serena. However, the tsunami was of low impact because the wave reached just a height of 4.5 m (Fig. 15).

5 Conclusions

The geomorphological characteristics of the studied catchments demonstrate the dynamic action of water and the favorable conditions for surface runoff. In both catchments, the topography and the substrates favor surface runoff and river flooding.

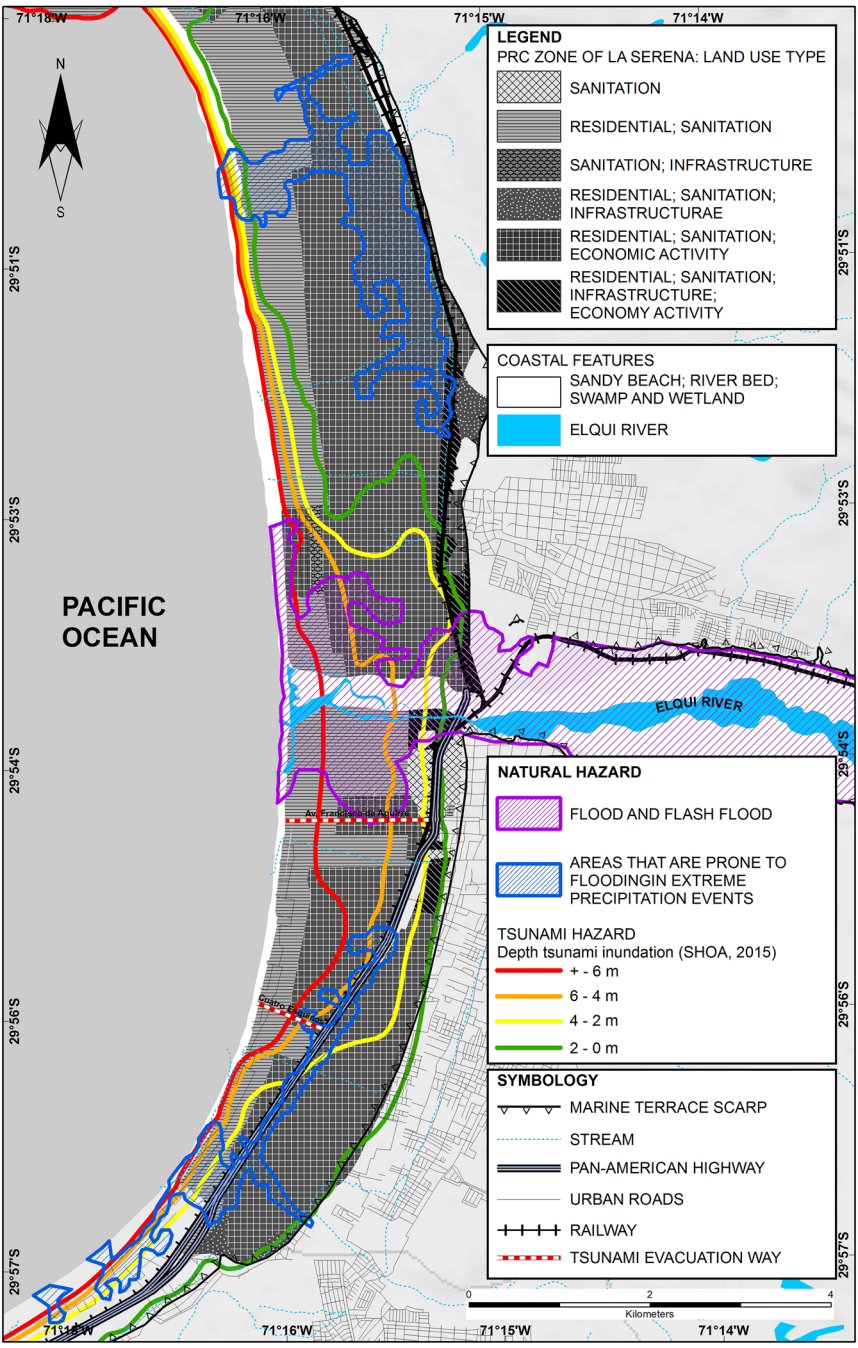

Fig. 15 Current and potential hazard and risk associated with urban growth process: Land use accepted by urban planning instruments (PRC) and risk areas related to rain fall events, fluvial floods and tsunamis

The available sediments on the slopes of the tributaries lead to high sediment discharges in the form of hyper-concentrated flows in the upper catchments as documented by evidences in the field. The supply of sediments is enhanced by a relatively high recurrence of large magnitude ($M > 6$) earthquakes in the region causing landslides.

The use of GIS proxies to morphometric analysis of catchments for susceptibility assessment expresses the existence of favorable conditions for occurrence of hydromorphologic processes such as flash floods and river floods in the studied catchments.

Due to climatic conditions, the fluvial systems are only sporadically active. It was estimated that precipitation events of more than 60 mm/24 h are triggering hydrometeorological processes with a decadal return period. Despite the 2015 rainfall events, there are morphologic, topographic and soil conditions for floods in the urban area associated with ENSO or another type of atmospheric phenomena with a 60-mm threshold, as well as with lower precipitation amounts, that can trigger floods in the urban areas in the coastal zone. Hence, the worst hazard and risk scenario might be an earthquake and an El Niño event working together.

Acknowledgements This work was funded by FONDECYT (National Fund for Science and Technology) projects 1120234 and 11130629. Special thanks to Giuliano Rodolfi, colleague and friend, who died in November 2015.

References

Araya-Vergara JF (1985) Análisis de la carta geomorfológica de la cuenca del Mapocho. Informaciones Geográficas 32:31–44

Aubrecht C, Fuchs S, Neuhold C (2013) Spatio-temporal aspects and dimensions in integrated disaster risk management. Nat Hazards 68:1205–1216. doi:10.1007/s11069-013-0619-9

Banks JC, Camp JV, Mankowitz MD (2014) Adaptation planning for floods: a review of available tools. Nat Hazards 70:1327–1337. doi:10.1007/s11069-013-0876-7

Beck S, Barrientos S, Kausel E, Reyes M (1998) Source characteristics of historic earthquakes along the central Chile subduction zone. J S Am Earth Sci 11(2):115–129

Birkmann J, Cardona OD, Carreño ML, Barbat AH, Pelling M, Schneiderbauer S, Kienberger S, Keiler M, Alexander D, Zeil P, Welle T (2013) Framing vulnerability, risk and societal responses: the MOVE framework. Nat Hazards 67:193–211. doi:10.1007/s11069-013-0558-5

Boehner J, Koethe R, Conrad O, Gross J, Ringeler A, Selige T (2002) Soil Regionalisation by means of terrain analysis and process parameterisation. In: Micheli E, Nachtergaele F, Montanarella L (eds) Soil classification 2001. European soil Bureau, research report no. 7, EUR 20398 EN, Luxembourg, pp 213–222

Cardona OD (2009) Teoría del Riesgos y Desastres. Gestión Integral de Riesgos y Desastres. Curso de Educación Superior. Universidad Internacional de Florida

Castro CP, Ortiz J (2003) Expansión urbana y niveles de vulnerabilidad a amenazas naturales en una ciudad de tamaño medio: La Serena, Región IV de Coquimbo. In: Preoceedings, 51 Congreso Internacional de Americanista, Santiago de Chile

Castro CP, Soto MV, Fernandez R, Maerker M, Rodolfi G (2009) Impacto de la geodinámica actual del valle de Nantoco, cuenca del río Copiapó, asociado a la reconversión productiva. Revista de Geografía Norte Grande 42:81–99

Comisión Nacional de Medio Ambiente (CONAMA) (2006) Estudio de la variabilidad climática en Chile para el siglo XXI. Informe Final. Realizado por el Departamento de Geofísica, Universidad de Chile, Santiago de Chile

Conrad O (2006) SAGA—program structure and current state of implementation. In: Bohner J, McCloy KR, Strobl J (eds) SAGA analysis and modelling applications. Verlag Erich Goltze GmbH, Göttingen, pp 39–52

Dirección Meteorológica de Chile (2014) http://164.77.222.61/climatologia/

Doerr SH, Shakesby RA, Walsh RPD (2000) Soil water repellency: its causes, characteristics and hydrogeomorphological significance. Earth Sci Rev 51(1–4):33–65

Emparán C, Pineda G (2006) Geología del área Andacollo Puerto Aldea. Región de Coquimbo. Carta Geológica de Chile. Serie Geología Básica. N° 96. Servicio Nacional de Geología y Minería. Santiago de Chile

Estrategia Internacional para la Reducción de Desastres (EIRD) (2008) El cambio climático y la reducción del riesgo de desastres. Naciones Unidas-EIRD, Suiza

Garreaud R, Aceituno P, Muñoz R, Rojas M, Montecinos A (2008). El clima de Chile está cambiando. Comunicación del Proyecto ACT-19. Variabilidad climática en Chile: evaluación, interpretación y proyecciones. Universidad de Chile. Santiago de Chile

Grohmann CH (2004) Morphometric analysis in geographic information systems: applications of free software GRASS and R. Comput Geosci 30(9–10):1055–1067. doi:10.1016/j.cageo.2004.08.002

Hawkins RH, Ward TJ, Woodward DE, Van Mullem JA (2009) Curve number hydrology—state of the practice. American Society of Civil Engineers (ASCE), Reston, VA

Huang SL, Yeh CT, Chang LF (2010) The transition to an urbanizing world and the demand for natural resources. Curr Opin Environ Sustain 2:136–143. doi:10.1016/j.cosust.2010.06.004

Instituto Nacional de Estadísticas (INE) (2012) Compendio Nacional de estadísticas. http://www.ine.cl/canales/menu/publicaciones/compendio_estadistico/compendio_estadistico2012.php

Kappes MS, Gruber K, Frigerio S, Bell R, Keiler M, Glade T (2012) The MultiRISK platform: the technical concept and application of a regional-scale multihazard exposure analysis tool. Geomorphology 151–152:139–155. doi:10.1016/j.geomorph.2012.01.024

Keiler M, Kellerer-Pirklbauer A, Otto JC (2012) Concepts and implications of environmental change and human impact: studies from Austrian geomorphological research (Preface). Geogr Ann 94:1–5. doi:10.1111/j.1468-0459.2012.00457.x

Le Roux JP, Vargas G (2005) Hydraulic behavior of tsunami backflows: insights from their modern and ancient deposits. Environ Geol 49:65–75

Le Roux JP, Olivares DM, Nielsen SN, Smith ND, Middleton H, Fenner J, Ishman SE (2006) Bay sedimentation as controlled by regional crustal behaviour, local tectonics and eustatics sea-level changes: Coquimbo Formation (Mioceno–Plioceno), Bay of Tongoy, central Chile. Sedyment Geol 184:133–153

Lei Y, Wang J (2014) A preliminary discussions on the opportunities and challenges of linking climatic changes adaptation with risk reduction. Nat Hazards 71:1587–1597. doi:10.1007/s11069-013-0966-6

Märker M, Castro CP, Pelacani S, Soto MV (2008) Assesment of degradation susceptibility in the Chacabuco Province of central Chile using a morphometric based response units approach. Geografia Física e Dinamica Quaternaria 31:47–53

Märker M, Pelacani S, Schröder B (2011) A functional entity approach to predict soil erosion processes in a small Plio-Pleistocene Mediterranean catchment in Northern Chianti, Italy. Geomorphology 125(4):530–540

Märker M, Dangel F, Soto Bäuerle V, Rodolfi G (2012) Assessment of natural hazards and vulnerability in the Rio Copiapó catchment: a case study in the ungauged Quebrada Cinchado Catchment. Investigaciones Geográficas Chile 44:17–28

Mitas L, Mitasova H (1998) Distributed soil erosion simulation for effective erosion prevention. Water Resour Res 34:505–516

Montgomery DR, Dietrich WE (1994a) Landscape dissection and drainage area-slope thresholds. In: Kirkby MJ (ed) Process models and theoretical geomorphology. Wiley, Hoboken

Montgomery DR, Dietrich WE (1994b) A physically-based model for the topographic control of shallow landsliding. Water Resour Res 30:1153–1171

Moscoso R, Nasi C, Salinas P (1982) Hoja de Vallenar y parte norte de La Serena. Escala 1:250.000. Servicio Nacional de Geología y Minería, Santiago de Chile

Oficina Nacional de Emergencias (ONEMI) (2015) http://www.onemi.cl/wp-content/themes/onemi-bootstrap-master/busqueda.html?search=tsunami+coquimbo+2015

Olaya V, Conrad O (2009) Geomorphometry in SAGA. In: Hengl T, Reuter HI (eds) Geomorphometry concpets, software, applications. Developments in soil science, vol 33. Elsevier, Amsterdam, NL, pp 293–308

Ortiz J, Escolano S (2005) Crecimiento periférico del Gran Santiago. Hacia la desconcentración funcional de la ciudad. http://www.ub.es/geocrit/sn/sn-194-04.htm

Ortiz J, Castro CP, Escolano S (2002) Procesos de reestructuración urbana y niveles de vulnerabilidad a amenazas naturales en una ciudad de tamaño medio del sistema urbano chileno: el caso de La Serena, en la Región IV de Coquimbo. Investigaciones Geográficas 36:17–42

Ortiz W, Castro CP, Rugiero V (2011) Percepción del riesgo en la comuna de la Serena. Revista INVI 75:105–142

Owen JJ, Amundson R, Dietrich WE, Nishiizumi K, Sutter B, Chong G (2011) The sensitivity of hillslope bedrock erosion to precipitation. Earth Surf Process Landf 36:117–135. doi:10.1002/esp.2083

Pardo M, Comte D, Monfre T (2002a) Seismotectonic and stress distribution in the central Chile subduction zone. J S Am Earth Sci 15:11–22

Pardo M, Comte D, Monfret T, Boroschek R, Astroza M (2002b) The October 15, 1997 Punitaqui earthquake (Mw = 7.1): a destructive event within the subducting Nazca plate in central Chile. Tectonophysics 345:199–210

Paskoff R (1970) Recherches geomorphologiques dans le Chili semi-aride. Biscaye Frères, Bordeaux

Renard KG, Foster GR, Weesies GA, McCool DK, Yoder DC (1997) Prediction soil erosion by water: a guide to conservation planning with the revised universal soil loss equation. Agricultural handbook 703. US Department of Agriculture, Washington, DC, p 404

Saillard M, Hall SR, Audin L, Fraber DL, Herail G, Martinod J, Regard V, Finkel RC, Bondoux F (2009) Non-steady long-term uplift rates and Pleistocene marine terrace development along the Andean margin of Chile (31°S) inferred from 10Be dating. Earth Planet Sci Lett 277:50–63

Saillard M, Riotte J, Regards V, Viollete A, Hérail G, Riquelme R (2011) Beach ridges UeTH dating in Tongoy bay tectonic implications for a peninsula bay system, Chile. J S Am Earth Sci 40:77–84

Sarricolea P (2004) Niveles de vulnerabilidad a amenazas naturales en una ciudad intermedia y sus áreas de expansión: el caso de la Serena, IV región de Coquimbo. Dissertation, Universidad de Chile

Sarricolea P, Martín-Vide J (2012) Distribución espacial de las precipitaciones diarias en Chile mediante el índice de concentración a resolución de 1 mm, entre 1965–2005. In: Cuadrat JM, Dorta MJ, Estrela F, González Rouco JA, López Díaz JC, García Codrón F, Sánchez Rodrigo J, Martín-Vide J, García Herrera R (eds) Cambio climático, extremos e impactos. Publicaciones de la Asociación Española de Climatología, Salamanca, pp 631–639

Sarricolea P, Herrera-Ossandon M, Meseguer-Ruiz O (2016) Climatic regionalisation of continental Chile. J Maps. doi:10.1080/17445647.2016.1259592

Soto MV (2016) Assessment of process dynamics and evolutionary trend of the western part of the arid Chilean coastal range: relationships between river catchments and coastal dynamics of the Coquimbo bay system, Chile. PhD Thesis, Eberhard Karls Universitat Tubingen

Soto MV, Märker M, Arriagada J, Castro CP, Rodolfi G (2010) Evaluación de la amenaza natural en ambiente semiárido, sustentada en la geomorfología y el modelamiento de índices topográficos. Salamanca, Región de Coquimbo, Chile. Investigaciones Geográficas 42:19–36

Soto MV, Märker M, Castro CP, Rodolfi G (2012) Dinámica actual de microcuencas del desierto costero de Atacama y su influencia en la generación de amenazas. Geografía Fisica e Dinámica Quaternaria 35:79–89

Soto MV, Märker M, Rodolfi G, Sepúlveda SA, Cabello M (2014) Assessment of geomorphic processes affecting the paleo-landscape of Tongoy Bay, Coquimbo Region, central Chile. Geografía Fisica e Dinámica Quaternaria 37:51–66

Soto MV, Märker M, Castro CP, Rodolfi G (2015) Análisis integrado de las condiciones de amenaza natural en el medio ambiente costero semiárido de Chile. La Serena, Coquimbo. Boletín de la Sociedad de Geógrafos de España 67:213–231

Tucker GE, Hancock GR (2010) Modelling landscape evolution. Earth Surf Proc Land 35:28–50

Vargas X (1999) Corrientes de detritos en la Quebrada de Macul, Chile. Estudio de caudales máximos. Ingeniería del Agua 6(4):341–344

Vigny C, Rudloff A, Ruegg JC, Madariaga R, Campos J, Alvarez M (2009) Upper plate deformation measured by GPS in the Coquimbo Gap, Chile. Phys Earth Planet Inter 175:86–95. doi:10.1016/j.pepi.2008.02.013

Wilcox DP, Sorice MG, Young MH (2011) Dryland ecohydrology in the anthropocene: taking stock of human–ecological interactions. Geogr Compass 5(3):112–127. doi:10.1111/j.1749-8198.2011.00413.x

Wyndam K (2012) Análisis de la vulnerabilidad y riesgo del sector turístico y la población flotante en la comuna de La Serena frente a la ocurrencia de una amenaza de origen natural. IV Región de Coquimbo. Dissertation, Universidad de Chile

Zakerinejad R, Märker M (2014) Prediction of Gully erosion susceptibilities using detailed terrain analysis and maximum entropy modeling: a case study in the Mazayejan Plain, Southwest Iran. Geografia Fisica e Dinamica Quaternaria 37(1):67–76. doi:10.4461/GFDQ.2014.37.7